

On the modelling of compressible inviscid flow problems using AUSM schemes

M. Hajžman^{a,*}, O. Bublík^a, J. Vimmr^a

^aDepartment of Mechanics, Faculty of Applied Sciences, UWB in Pilsen, Univerzitní 22, 306 14 Plzeň, Czech Republic

Received 7 September 2007; received in revised form 10 October 2007

Abstract

During last decades, upwind schemes have become a popular method in the field of computational fluid dynamics. Although they are only first order accurate, AUSM (Advection Upstream Splitting Method) schemes proved to be well suited for modelling of compressible flows due to their robustness and ability of capturing shock discontinuities. In this paper, we review the composition of the AUSM flux-vector splitting scheme and its improved version noted AUSM+, proposed by Liou, for the solution of the Euler equations. Mach number splitting functions operating with values from adjacent cells are used to determine numerical convective fluxes and pressure splitting is used for the evaluation of numerical pressure fluxes. Both versions of the AUSM scheme are applied for solving some test problems such as one-dimensional shock tube problem and three-dimensional GAMM channel. Features of the schemes are discussed in comparison with some explicit central schemes of the first order accuracy (Lax-Friedrichs) and of the second order accuracy (MacCormack).

© 2007 University of West Bohemia. All rights reserved.

Keywords: compressible flow, Euler equations, AUSM scheme, flux-vector splitting, shock tube problem, 3D GAMM channel

1. Introduction

The growth of interest in computational fluid dynamics in 1980s brought the development of sufficiently robust, accurate and efficient numerical methods. Especially, upwind schemes proved to be efficient for the solution of compressible inviscid flow problems described by the non-linear system of the Euler equations. Recently, upwind schemes have become well-used for their accuracy with regard to other first order accurate schemes (e.g. central explicit Lax-Friedrichs scheme) and for their capability of capturing shock and contact discontinuities in a wide variety of problems.

In 1990, the AUSM scheme was presented as a simple, first order accurate and robust method in comparison with existing numerical schemes and became early one of the most used computational fluid dynamics techniques. Several attempts have been made in the following years to improve the original AUSM scheme proposed by Liou and Steffen, [5]. Various types of flux splittings, [4], have been tested to increase accuracy and to reduce numerical diffusion. Various versions of the AUSM-family schemes have been written into numerical codes.

In this paper, we review the finite volume formulation of the first order accurate AUSM scheme proposed by Liou and Steffen, [5]. Secondly, we mention an improved AUSM+ scheme, [3], having following features: exact resolution of stationary shock discontinuities, positivity

*Corresponding author. Tel.: +420 377 632 394, e-mail: hajzmanm@kme.zcu.cz.

preserving of scalar quantity such as the density, improved accuracy with regard to its predecessor AUSM and other popular schemes, simplicity and easy generalization to other conservation laws. In order to improve the accuracy, Mach number and pressure splitting functions are used in these AUSM schemes. Necessary mathematical properties of these splitting functions and detailed steps in the construction of the schemes are also mentioned in the paper.

The main contribution is creation of the software based on the finite volume formulation of the AUSM and AUSM+ schemes on a structured grid and its application for the solution of test problems. Firstly, features of the schemes are shown on the shock tube problem. The results are analyzed in comparison with the exact solution and with results obtained by well-known central schemes of the first and second order accuracy. Three-dimensional inviscid transonic flow through the 3D GAMM channel is also considered and the results obtained by the AUSM+ scheme are compared with the numerical solution achieved by the central second order accurate two-step MacCormack scheme.

2. Mathematical model

The mathematical model of a compressible inviscid fluid flow is described by the non-linear conservative system of the Euler equations. In the two-dimensional Cartesian coordinate system, the hyperbolic system of the Euler equations can be expressed by

$$\frac{\partial \mathbf{W}}{\partial t} + \frac{\partial \mathbf{f}(\mathbf{W})}{\partial x} + \frac{\partial \mathbf{g}(\mathbf{W})}{\partial y} = \mathbf{0}, \quad (1)$$

where x, y are the Cartesian coordinates, t is time, $\mathbf{W} = [\rho, \rho u, \rho v, \rho E]^T$ is the vector of conservative variables and $\mathbf{f}(\mathbf{W}) = [\rho u, \rho u^2 + p, \rho uv, \rho uH]^T$, $\mathbf{g}(\mathbf{W}) = [\rho v, \rho uv, \rho v^2 + p, \rho vH]^T$ are the Cartesian components of the inviscid flux $\mathbf{F}(\mathbf{W}) = (\mathbf{f}(\mathbf{W}), \mathbf{g}(\mathbf{W}))^T$. In these expressions, ρ is the density, p is the static pressure, E is the total energy per unit mass, $\mathbf{v} = (u, v)^T$ is the velocity vector and H is the enthalpy. The relation between the enthalpy and the total energy can be written as $H = E + p/\rho$. The conservative system of the Euler equations (1) has to be completed with an equation of state $p = p(\rho, T)$, where T is the thermodynamical temperature. For the inviscid compressible flow with ideal gas properties, the static pressure p can be expressed by the constitutive relation

$$p = (\kappa - 1) \left[\rho E - \frac{1}{2} \rho (u^2 + v^2) \right], \quad (2)$$

where κ is the Poisson's ratio.

3. Numerical method

In this section, we will firstly show the finite volume formulation of the upwind scheme. Then we will focus on the detailed description of the process which leads to the determination of numerical fluxes in both AUSM and AUSM+ schemes. Mathematical properties of splitting functions, that are used to improve accuracy of the schemes, will be also mentioned.

3.1. Finite volume discretization of the Euler equations

For the discretization of the conservative system of the Euler equations (1), the cell-centered finite volume method on a structured quadrilateral grid was used. In this method, the computational domain $\Omega \in \mathbb{R}^2$ is subdivided into a finite number of non-overlapping quadrilateral

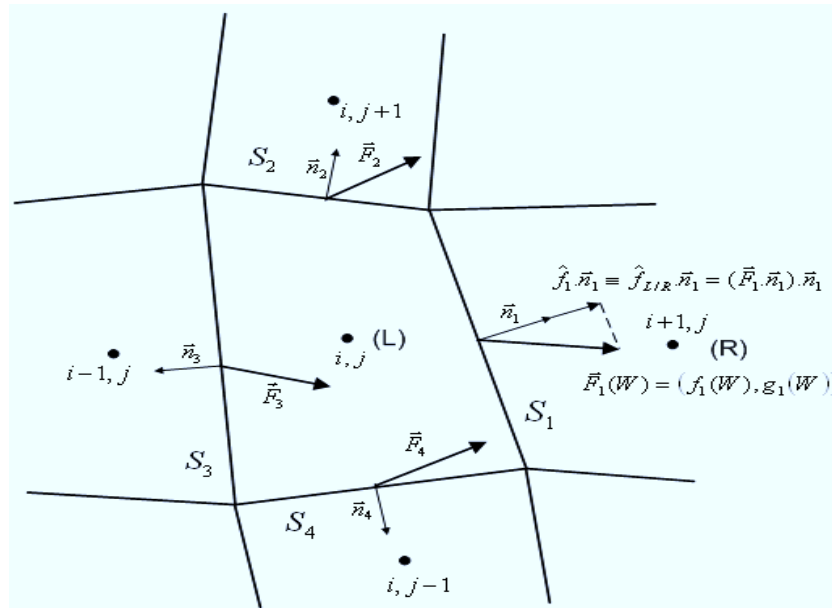


Fig. 1. Finite volume \$\Omega_{ij}\$ and AUSM fluxes through its faces.

finite volumes \$\Omega_{ij}\$ with the boundary \$\partial\Omega_{ij}\$, [1]. Integrating of (1) over \$\Omega_{ij}\$ and applying the Gauss-Ostrogradski's Theorem to this system we obtain

$$\frac{\partial}{\partial t} \int_{\Omega_{ij}} \mathbf{W} d\Omega_{ij} + \oint_{\partial\Omega_{ij}} (n_x \mathbf{f} + n_y \mathbf{g}) dS = 0, \quad (3)$$

where \$n_x\$ and \$n_y\$ are the Cartesian components of the unit vector normal to the boundary \$\partial\Omega_{ij}\$. Substituting the first integral on the left side of (3) by \$\overline{\mathbf{W}}_{ij} \cdot |\Omega_{ij}|\$, where \$\overline{\mathbf{W}}_{ij}\$ is the integral average of \$\mathbf{W}\$ over \$\Omega_{ij}\$ and \$|\Omega_{ij}|\$ is the area of the cell \$\Omega_{ij}\$, we get

$$\frac{d\overline{\mathbf{W}}_{ij}}{dt} \cdot |\Omega_{ij}| + \oint_{\partial\Omega_{ij}} (n_x \mathbf{f} + n_y \mathbf{g}) dS = 0. \quad (4)$$

Substituting the time derivation of \$\overline{\mathbf{W}}_{ij}\$ by a difference formula of the first order accuracy and the integral in (4) by a sum of numerical fluxes, together with the notation \$\overline{\mathbf{W}}_{ij} \equiv \mathbf{W}_{ij}\$ we get

$$\mathbf{W}_{ij}^{n+1} = \mathbf{W}_{ij}^n - \frac{\Delta t}{|\Omega_{ij}|} \cdot \sum_{k=1}^4 \hat{f}_k S_k, \quad (5)$$

where \$\hat{f}_k\$ are numerical fluxes through the appropriate edge of the quadrilateral control volume \$\Omega_{ij}\$ and \$S_k\$ are the edge lengths, e.g. \$\hat{f}_1 \equiv \hat{f}_{L/R}\$ in fig. 1. The numerical fluxes through each face of the control volume can be written as combinations of convective and pressure terms

$$\hat{f} = n_x \mathbf{f} + n_y \mathbf{g} = V_n \begin{pmatrix} \rho \\ \rho u \\ \rho v \\ \rho H \end{pmatrix} + p \begin{pmatrix} 0 \\ n_x \\ n_y \\ 0 \end{pmatrix} = \hat{f}^c + p \begin{pmatrix} 0 \\ n_x \\ n_y \\ 0 \end{pmatrix}, \quad (6)$$

where \$V_n = un_x + vn_y\$ is the convective velocity normal to the appropriate interface. There is a number of ways how to compute the numerical fluxes in AUSM schemes. The description of such processes in AUSM and AUSM+ schemes is given below.

3.2. AUSM scheme

The first step in the construction of AUSM fluxes is to compute the interface-normal Mach numbers for the left and right cells corresponding to each face of the control volume. We consider

$$M_L = \frac{\vec{V}_L \cdot \vec{n}}{a_L}, \quad M_R = \frac{\vec{V}_R \cdot \vec{n}}{a_R}, \quad (7)$$

where a_L, a_R are values of the speed of sound, \vec{V}_L, \vec{V}_R are the velocity vectors in the left and right cells, \vec{n} is the unit vector normal to the appropriate face and (\cdot) denotes the scalar product of two vectors. Values from (7) play an important role in determining the interface Mach number

$$M_{L/R} = \mathcal{M}^+(M_L) + \mathcal{M}^-(M_R), \quad (8)$$

where \mathcal{M}^+ and \mathcal{M}^- are the Mach number splitting functions. These functions are used in the AUSM schemes to improve their accuracy. We require that they satisfy following properties, [3]:

- (M1) $\mathcal{M}^+(M) + \mathcal{M}^-(M) = M$, for consistency.
- (M2) $\mathcal{M}^+(M) \geq 0$ and $\mathcal{M}^-(M) \leq 0$.
- (M3) \mathcal{M}^\pm are monotone increasing functions of M .
- (M4) $\mathcal{M}^+(M) = -\mathcal{M}^-(-M)$, i.e., a symmetry property.
- (M5) $\mathcal{M}^+(M) = M$ as $M \geq 1$; $\mathcal{M}^-(M) = M$ as $M \leq -1$.
- (M6) \mathcal{M}^\pm are continuously differentiable.

In this paper we will consider Mach number splitting functions in the form, [6],

$$\mathcal{M}^\pm(M) = \begin{cases} \frac{1}{2}(M \pm |M|), & \text{if } |M| > 1, \\ \pm \frac{1}{4}(M \pm 1)^2 \pm \frac{1}{8}(M^2 - 1)^2, & \text{otherwise.} \end{cases} \quad (9)$$

The pressure term is obtained similarly as the interface Mach number considering

$$p_{L/R} = \mathcal{P}^+(M_L) \cdot p_L + \mathcal{P}^-(M_R) \cdot p_R, \quad (10)$$

where p_L, p_R are values of the static pressure in the left and right cells. The pressure splitting functions \mathcal{P}^\pm must satisfy following six properties, [3]:

- (P1) $\mathcal{P}^+(M) + \mathcal{P}^-(M) = 1$, for consistency.
- (P2) $0 \leq \mathcal{P}^\pm(M)$ as required by the physical constraint that the pressure be nonnegative.
- (P3) $\partial \mathcal{P}^+ / \partial M \geq 0$ and $\partial \mathcal{P}^- / \partial M \leq 0$.
- (P4) $\mathcal{P}^+(M) = \mathcal{P}^-(-M)$.
- (P5) $\mathcal{P}^+(M) = 1$ as $M > 1$; $\mathcal{P}^-(M) = 1$ as $M < -1$.
- (P6) $\mathcal{P}^\pm(M)$ are continuously differentiable.

In the case of the AUSM scheme, following pressure splitting functions were used, [3],

$$\mathcal{P}^\pm(M) = \begin{cases} \frac{1}{2}(M \pm |M|)/M, & \text{if } |M| > 1, \\ \frac{1}{4}(M \pm 1)^2(2 \mp M), & \text{otherwise.} \end{cases} \quad (11)$$

Consequently, the convective term of the numerical flux through a cell interface can be written as

$$\hat{\mathbf{f}}_{L/R}^c = \begin{cases} M_{L/R} \cdot \hat{\mathbf{f}}_L^c, & \text{if } M_{L/R} \leq 0, \\ M_{L/R} \cdot \hat{\mathbf{f}}_R^c, & \text{if } M_{L/R} > 0, \end{cases} \quad \text{where } \hat{\mathbf{f}}_{L(R)}^c = \begin{pmatrix} \rho a \\ \rho a u \\ \rho a v \\ \rho a H \end{pmatrix}_{L(R)}. \quad (12)$$

The total AUSM flux through a cell face can be finally expressed by the formula

$$\hat{\mathbf{f}}_{L/R} = \frac{1}{2}M_{L/R}(\hat{\mathbf{f}}_L^c + \hat{\mathbf{f}}_R^c) - \frac{1}{2}|M_{L/R}|(\hat{\mathbf{f}}_R^c - \hat{\mathbf{f}}_L^c) + p_{L/R} \begin{pmatrix} 0 \\ n_x \\ n_y \\ 0 \end{pmatrix}. \quad (13)$$

3.3. AUSM+ scheme

The process of determining numerical fluxes in the AUSM+ scheme is similar to that in the AUSM scheme, and therefore, we will show only differences between these schemes. Firstly, the interface speed of sound is introduced using the arithmetic average of two neighbouring values, [6] or [3],

$$a_{L/R} = \frac{a_L + a_R}{2}. \quad (14)$$

Then the Mach number values in the left and right cell sides are given by the relations

$$M_L = \frac{\vec{V}_L \cdot \vec{n}}{a_{L/R}}, \quad M_R = \frac{\vec{V}_R \cdot \vec{n}}{a_{L/R}}. \quad (15)$$

The interface Mach number $M_{L/R}$ is determined by the equation (8), where the Mach number splitting functions (9) are considered. The interface pressure $p_{L/R}$ is obtained using (10), but the pressure splitting functions \mathcal{P}^\pm are determined by, [6],

$$\mathcal{P}^\pm(M) = \begin{cases} \frac{1}{2}(1 \pm \text{sign}(M)), & \text{if } |M| \geq 1, \\ \frac{1}{4}(M \pm 1)^2(2 \mp M) \pm \frac{3}{16}(M^2 - 1)^2, & \text{otherwise.} \end{cases} \quad (16)$$

The final form of the AUSM+ numerical flux through a cell face is

$$\hat{\mathbf{f}}_{L/R} = \frac{1}{2}M_{L/R} a_{L/R}(\hat{\mathbf{f}}_L^c + \hat{\mathbf{f}}_R^c) - \frac{1}{2}|M_{L/R}| a_{L/R}(\hat{\mathbf{f}}_R^c - \hat{\mathbf{f}}_L^c) + p_{L/R} \begin{pmatrix} 0 \\ n_x \\ n_y \\ 0 \end{pmatrix}, \quad (17)$$

where the convective flux is considered as $\hat{\mathbf{f}}_{L(R)}^c = [\rho, \rho u, \rho v, \rho H]_{L(R)}^T$.

4. Applications and numerical results

4.1. The shock tube problem

The shock tube problem is a case of shock waves propagation in a one-dimensional tube and is often used for testing various numerical methods, [1]. An important reason for us to choose this problem as an example is that its exact analytical solution is known, [1]. Thus, it is very easy to compare numerical results with the analytical solution and to judge the accuracy of the numerical solution.

We assume a one-dimensional tube, where $x \in < 0; 1 >$, with a diaphragm initially located in $x = 0.5$ separating two different states of gas. We study the time evolution of this problem after removing the diaphragm. Following initial conditions in the dimensionless form have been adopted:

- $p = 1, \rho = 1, u = 0$ for $x \leq 0.5$,
- $p = 0.1, \rho = 0.125, u = 0$ for $x > 0.5$.

In all figures given below, the obtained numerical results are compared with the exact solution. In fig. 2, fig. 3 and fig. 4, we can see comparisons of the numerical solutions computed by two schemes of the first order accuracy - the upwind AUSM scheme and the well-known central Lax-Friedrichs scheme. From these figures, it is obvious that the AUSM scheme gives better

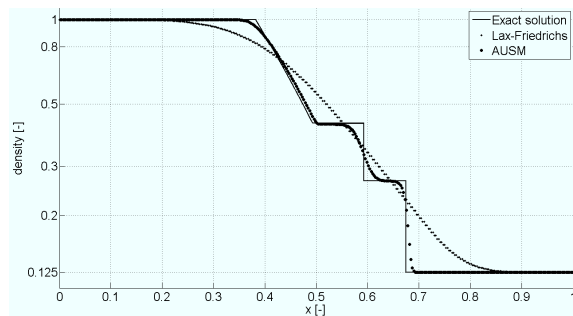


Fig. 2. Density distributions in the shock tube obtained using Lax-Friedrichs and AUSM schemes together with the exact solution.

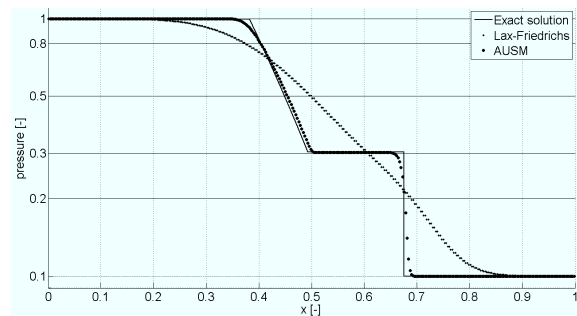


Fig. 3. Pressure distributions in the shock tube obtained using Lax-Friedrichs and AUSM schemes together with the exact solution.

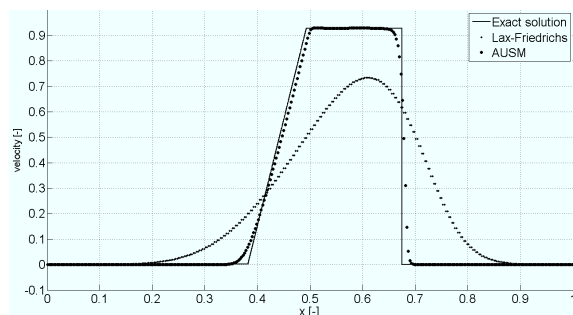


Fig. 4. Velocity distributions in the shock tube obtained using Lax-Friedrichs and AUSM schemes together with the exact solution.

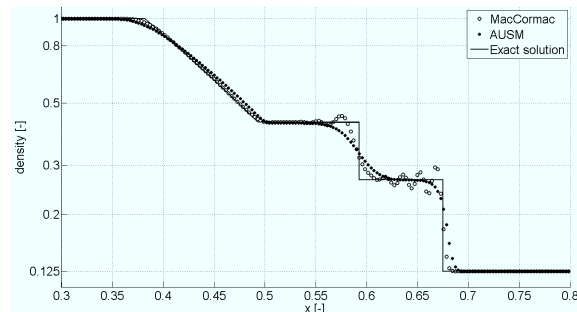


Fig. 5. Density distributions in the shock tube obtained by the MacCormack scheme with Jameson's artificial viscosity and the AUSM scheme together with the exact solution.

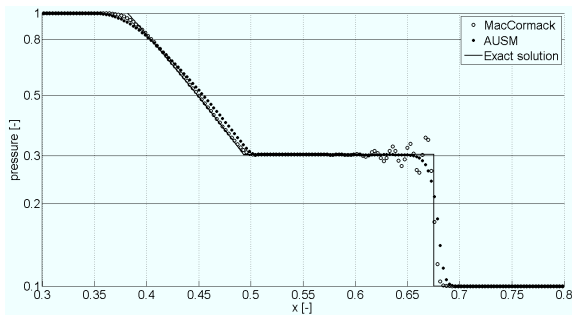


Fig. 6. Pressure distributions in the shock tube obtained by the MacCormack scheme with Jameson's artificial viscosity and the AUSM scheme together with the exact solution.

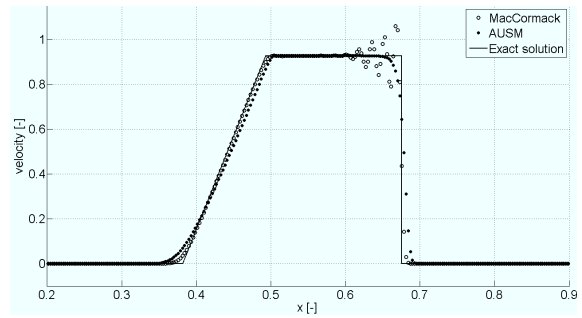


Fig. 7. Velocity distributions in the shock tube obtained by the MacCormack scheme with Jameson's artificial viscosity and the AUSM scheme together with the exact solution.

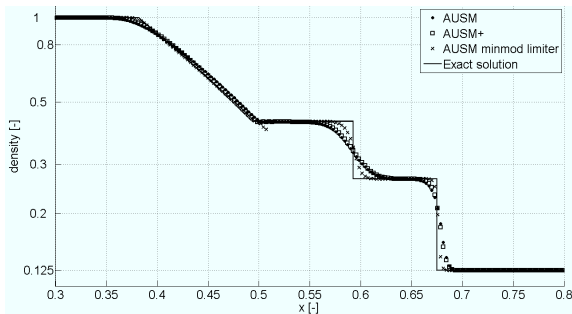


Fig. 8. Density distributions in the shock tube obtained using AUSM, AUSM+ and AUSM with *minmod* limiter schemes together with the exact solution.

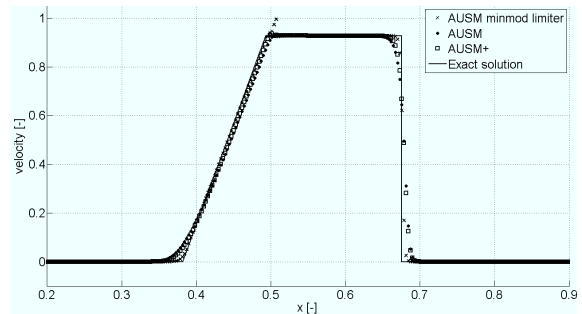


Fig. 9. Velocity distributions in the shock tube obtained using AUSM, AUSM+ and AUSM with *minmod* limiter schemes together with the exact solution.

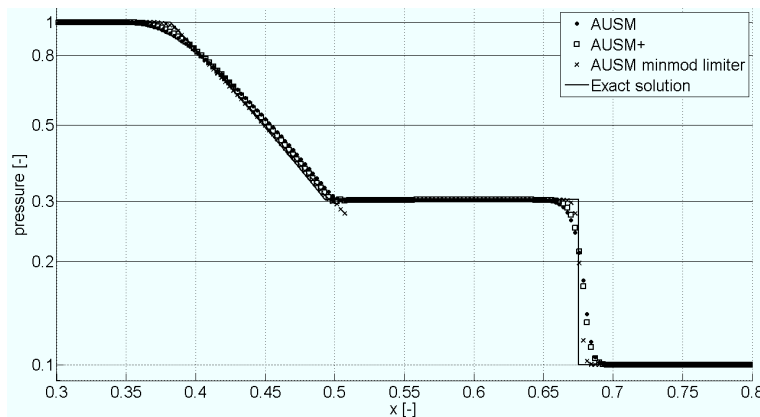


Fig. 10. Pressure distributions in the shock tube obtained using AUSM, AUSM+ and AUSM with *minmod* limiter schemes together with the exact solution.

results, especially in the vicinity of shock and contact discontinuities. Another comparisons are made in fig. 5, fig. 6 and fig. 7, where the results obtained using the AUSM scheme and the explicit two-step MacCormack scheme of the second order accuracy are shown. We can see that the central MacCormack scheme gives more accurate results than the AUSM scheme,

but it produces oscillations near shock and contact discontinuities. In order to reduce these oscillations, the Jameson's artificial viscosity, [7], was added to the scheme with coefficients $\alpha_2 = 0.8$ and $\alpha_4 = 0.03$. The last comparison is made in fig. 8, fig. 9, fig. 10, where the results obtained using the AUSM scheme, the AUSM+ scheme and the improved second order accurate AUSM scheme with the *minmod* limiter, [8] and [2], are shown. From these figures, we can see that the AUSM+ scheme gives somewhat better results than the original AUSM scheme, but the most accurate results were obtained using the improved AUSM scheme with *minmod* limiter.

4.2. The 3D GAMM channel

As the second test problem, the transonic flow of inviscid fluid through the three-dimensional GAMM channel was considered. Geometry of this channel with the obstacle is shown in fig. 11. The computational domain was discretized by a structured hexahedral grid consisting of $200 \times 50 \times 21$ cells illustrated in fig. 12.

Following boundary conditions were prescribed at the inlet section for the subsonic case:

- dimensionless value of total pressure $\bar{p}_0 = 1$ corresponding to $p_0 = 1.37483 \cdot 10^5$ Pa,
- dimensionless value of total density $\bar{\rho}_0 = 1$ corresponding to $\rho_0 = 1.4637$ kg m⁻³,
- two inlet stream angles $\varphi = 0^\circ$ and $\psi = 90^\circ$.

At the outlet boundary, only one condition was prescribed for the subsonic case:

- dimensionless value of static pressure $\bar{p}_2 = 0.737$ corresponding to the real value of $p_2 = 1.01325 \cdot 10^5$ Pa.

For the numerical solution of the problem of inviscid transonic flow through the three-dimensional GAMM channel, the first order accurate AUSM+ scheme was used. In this paper, the numerical results obtained by this scheme are compared with the results obtained by the second order accurate, explicit two-step MacCormack scheme with the Jameson's artificial viscosity. The coefficients in the dissipative term were chosen as $\alpha_2 = 0.75$ and $\alpha_4 = 0.045$, see [7].

Mach number distributions along the lower and upper channel walls for $z = 0$, $z = 0.5$ and $z = 1$ are shown in fig. 13, fig. 14 and fig. 15. It is obvious that the results obtained by the AUSM+ scheme are not as well as the results obtained by the MacCormack scheme. On the other hand the AUSM+ scheme captures the shock satisfactorily with regard to the second order accurate MacCormack scheme, even though it is only of first order accuracy. The first-order spatial accuracy of the AUSM+ scheme can be improved using a linear reconstruction with limiters, for more details see [2], [8], [1].

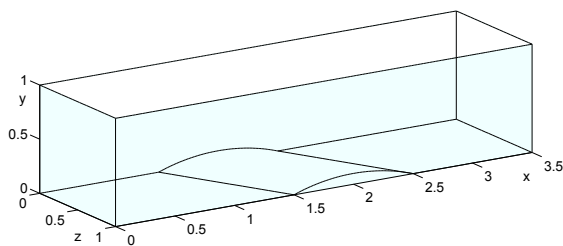


Fig. 11. Geometry of the 3D GAMM channel.

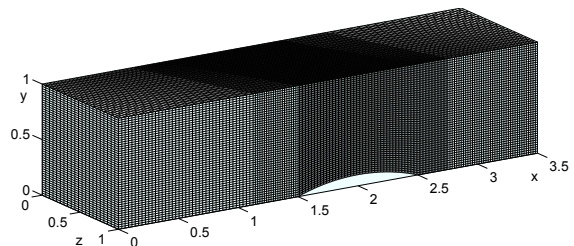


Fig. 12. Grid of the 3D GAMM channel.

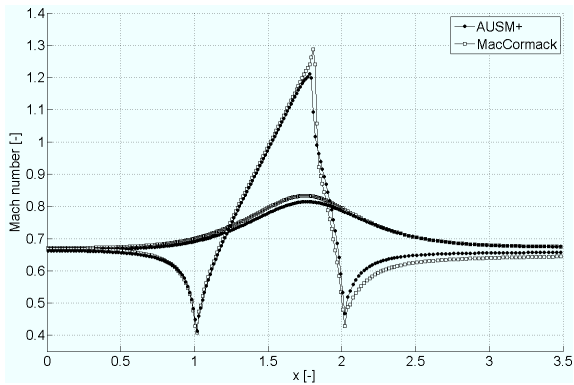


Fig. 13. Mach number distributions along the lower and upper walls of the 3D GAMM channel for $z = 0$ obtained using the AUSM+ and MacCormack schemes.

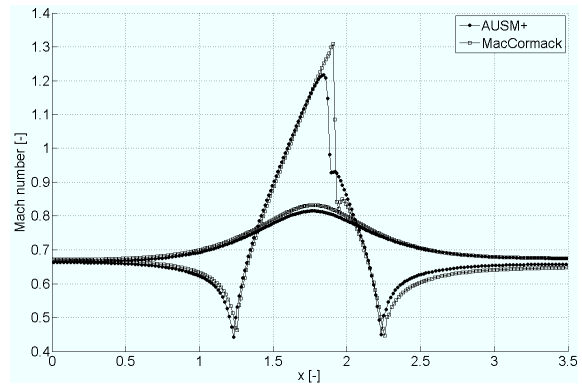


Fig. 14. Mach number distributions along the lower and upper walls of the 3D GAMM channel for $z = 0.5$ obtained using the AUSM+ and MacCormack schemes.

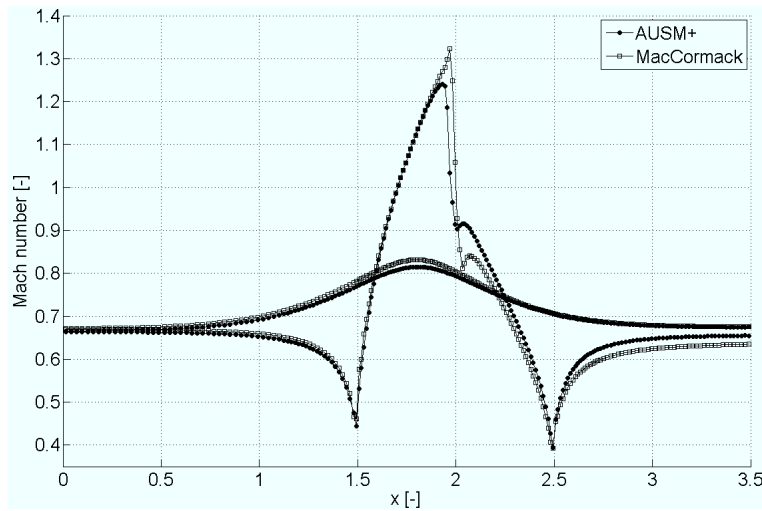


Fig. 15. Mach number distributions along the lower and upper walls of the 3D GAMM channel for $z = 1$ obtained using the AUSM+ and MacCormack schemes.

5. Conclusion

The advection upstream splitting method has recently become a popular computational method for solving problems of fluid dynamics, mainly due to its simplicity, robustness and ability of capturing shock and contact discontinuities. A number of various versions of AUSM schemes have been proposed since 1990. In this paper, the original AUSM scheme and its improved version AUSM+ proposed by Liou, [5], [3], were reviewed. These methods were applied on two test problems and the results were analyzed in comparison with the exact solution or with results obtained by other numerical schemes.

Considering the shock tube problem, we firstly compared two first order accurate schemes - the upwind AUSM and the central Lax-Friedrichs scheme. It is obvious that the AUSM scheme gives better results than the Lax-Friedrichs scheme and better captures shock and contact discontinuities. From the next comparison we can see that the central explicit two-step MacCor-

MacCormack scheme of the second order accuracy gives naturally better results than the AUSM scheme, however it produces oscillations in the numerical solution near shock and contact discontinuities leading to the application of the artificial viscosity. Then we analyzed results obtained by various versions of upwind schemes - AUSM, AUSM+ and AUSM scheme with improved accuracy using *minmod* limiter. The AUSM+ scheme proved to be more accurate than the original AUSM scheme, but the most accurate results were obtained using the second order accurate AUSM scheme with *minmod* limiter. For the solution of the transonic inviscid flow through the three-dimensional GAMM channel, the AUSM+ scheme was applied and the results were compared with results obtained using the central explicit two-step MacCormack scheme presented in [7]. It was shown that the results obtained by the MacCormack scheme with Jameson's artificial viscosity are more accurate than those obtained using the AUSM+ scheme.

Finally, we can say that the schemes from the AUSM-family proved to be more suitable for solving of transonic inviscid flow problems than, for example, the central first order accurate scheme such as Lax-Friedrichs scheme, particularly for their better capturing of shock and contact discontinuities. Naturally, numerical schemes from the AUSM family in their original forms are not as accurate as central explicit schemes of the second order accuracy such as the MacCormack scheme with the Jameson's artificial viscosity. Therefore, the improvement of their accuracy using a proper reconstruction with limiters, [2], is desired. This will be the object of our future interest.

Acknowledgements

This investigation was supported by the research project MSM 4977751303 of the Ministry of Education, Youth and Sports of the Czech Republic.

References

- [1] C. Hirsch, Numerical computation of internal and external flows, Vol. 1, 2, John Wiley & Sons, Chichester, 1990.
- [2] R.J. LeVeque, Finite volume methods for hyperbolic problems, Cambridge University Press, 2002.
- [3] M.-S. Liou, A sequel to AUSM: AUSM+, Journal of Computational Physics 256 (129) (1996) 364-382.
- [4] M.-S. Liou, Ten years in the making - AUSM family, 15th AIAA CFD Conference, AIAA Paper 2001-2521, 2001.
- [5] M.-S. Liou, C.J. Steffen, A new flux splitting scheme, Journal of Computational Physics 107 (1993) 23-39.
- [6] R.C. Ripley, F.-S. Lien, M.M. Yovanovich, Numerical simulation of shock diffraction on unstructured meshes, Computers & Fluids 35 (2006) 1420-1431.
- [7] J. Vimmr, Numerical computation of 3D inviscid transonic flow using MacCormack scheme with different artificial viscosity terms, Proceedings the 4th Scientific Conference Applied Mechanics, Ostrava, 2002, pp. 395-402.
- [8] M. Žaloudek, J. Fořt, J. Fürst, Numerical solution of compressible flow in a channel and blade cascade, Flow, Turbulence and Combustion 76 (2006) 353-361.